Formation of a Tornado and Its Breakdown (Coherent Vortical Structures : Their Roles in Turbulence Dynamics)

AUTHOR(S):

Komurasaki, Satoko; Kawamura, Tetsuya; Kuwabara, Kunio

CITATION:

Komurasaki, Satoko ...[et al]. Formation of a Tornado and Its Breakdown (Coherent Vortical Structures : Their Roles in Turbulence Dynamics). 数理解析研究所講究録 2000, 1121: 120-128

ISSUE DATE:

2000-01

URL:

http://hdl.handle.net/2433/63520

数理解析研究所講究録
1121 巻 2000 年 120-128

Formation of a Tornado and Its Breakdown

Ochanomizu University Satoko Komurasaki (小紫 誠子)
Ochanomizu University Tetuya Kawamura (河村 哲也)
ISAS Kunio Kuwahara (桑原 邦郎)

Natural convection caused by a confined heat source makes a strong concentration of vortices under Coriolis force. This is often observed as a fire tornado or a typhoon. We extensively studied these phenomena by solving the Navier-Stokes equations using a finite-difference method. We have found that under a certain condition the vortices strongly concentrate into a single vortex and the vortex breaks down. This is another example of a vortex breakdown. It is not known that this phenomenon happens in a real tornado or a typhoon, but it may occur. This makes a strong turbulent flow and an impinging jet onto the terrain, and may cause a disaster.

I. Introduction

Thermal convection is one of the most important phenomena in atmosphere which have deep relationship with daily life. It is caused by the density difference due to thermal expansion, and has been studied not only in meteorology but in physics and engineering.

Fire tornado caused by a big fire is an example of thermal convection. This problem is not merely basic but related with the calamity of the Great Kanto Earthquake. At 11:58 am, September 1st, 1923, the devastating earthquake happened in the central Tokyo area, and a number of fires occurred at various points in the city, then many people escaped from the combustion, gathering into the site of the former Army Clothing Depot which was a wide ground about 1 km in diameter. Then at 3:30 pm, a violent tornado broke out there, during which the mortality well exceeded forty thousands. The meteorological interpretation of this tragedy, which was believed among the academic circle, is the passage of a cold front. However, Soma[1] pointed out that the above interpretation involved some contradictions with the observed records, suggesting that the cause was simply a fire tornado induced by the big fire. Kuwahara et al.[2] showed numerically and experimentally that the main flow due to the convection from ring-type heat source was strongly concentrated within the central portion above the ring where no heat was supplied at the bottom, and suggested that big fire might accompany a big fire tornado, which might be the probable cause of the calamity of the Great Kanto Earthquake. Suito et al.[3] studied about fire tornado from big fire through numerical simulation with Hook-type heat source which was a simple model of the real disaster, and showed that the thermal flow from the heat source on the ground came into tornado only because of the thermal convection

with Coriolis force. However, this simulation was carried out in a small domain to compute relative to the size of the heat source, simulations in a larger domain are needed to investigate its real mechanism. On the other hand, Sato[4] investigated fire tornado based on reduced scale model experiments. There, the fire flame was surrounded by a vertical cylinder or square duct with slits to initiate the rotation of the flame. It sucked the ambient air through slits with variable guide vanes, and started to rotate. This study indicated that there was a possibility of the generation of rather localized fire tornado in the real urban area where some buildings stood in a shape for example U-type or L-type, than that from big fire like the calamity of the Great Kanto Earthquake.

It is important to simulate the big fire tornado in more realistic scale, to investigate its mechanism. Since it is impossible to do the real scale experiment, we have numerically studied about a fire tornado induced by a big fire. The computation with Hook-type heat source is done in a real scale. A realistic size of domain relative to the size of the heat source is employed to simulate. Conditions in this simulation are similar to that at the calamity of the Great Kanto Earthquake.

II. Computational method

The governing equations in this study are the compressible Navier-Stokes equations. In three-dimensional Descartes coordinates system, they are as follows:

$$\frac{1}{\rho}\left\{\frac{\partial \rho}{\partial t}+u_j\frac{\partial \rho}{\partial x_j}\right\}=-\frac{\partial u_j}{\partial x_j}, \tag{1}$$

$$\frac{\partial u_i}{\partial t}+u_j\frac{\partial u_i}{\partial x_j}=-\frac{1}{\rho}\frac{\partial p}{\partial x_i}+\frac{1}{\rho}\frac{\partial}{\partial x_j}\left\{\mu\left(\frac{\partial u_i}{\partial x_j}+\frac{\partial u_j}{\partial x_i}\right)\right\}+K_i \quad (i=1,2,3), \tag{2}$$

$$\frac{\partial \mathrm{C_v}T}{\partial t}+u_j\frac{\partial \mathrm{C_v}T}{\partial x_j}=\frac{1}{\rho}\frac{\partial}{\partial x_j}\left(\kappa\frac{\partial T}{\partial x_j}\right)-\frac{1}{\rho}p\frac{\partial u_j}{\partial x_j}. \tag{3}$$

μ : viscosity, κ : thermal diffusion coefficient,

$\boldsymbol{K}=(K_1,K_2,K_3)$: external force, $\mathrm{C_v}$: specific heat at constant volume.

Coriolis force is included in these equations as external force. The flow induced by the fire is considered to be slow enough that no shock waves appear in the flow field although the temperature difference is large. This means that these equations are solved under the assumption[5] that the pressure difference from the base pressure is small all over the field.

The equation of state for the perfect gas is

$$\rho=\frac{p}{\mathrm{R}T}.$$

Since the pressure is considered to be nearly constant as mentioned above, this equation can be written as follows:

$$\rho=\frac{1}{\alpha T} \quad \left(\alpha=\frac{\mathrm{R}}{p_m},\ p_m : \text{mean pressure}\right).$$

By substituting this equation into the left hand side of eq.(1), it becomes

$$\frac{1}{\rho}\frac{\mathrm{D}\rho}{\mathrm{D}t} = -\frac{1}{T}\frac{\mathrm{D}T}{\mathrm{D}t}. \tag{4}$$

Therefore, eq.(1) becomes

$$\frac{\partial u_j}{\partial x_j} = \frac{1}{T}\frac{\mathrm{D}T}{\mathrm{D}t}. \tag{5}$$

Putting eq.(5) into eq.(3),

$$\mathrm{C_p}\frac{\mathrm{D}T}{\mathrm{D}t} = \alpha T\frac{\partial}{\partial x_j}\left(\kappa\frac{\partial T}{\partial x_j}\right) \quad (\mathrm{C_p} = \mathrm{C_v} + \mathrm{R}) \tag{6}$$

is obtained. From eqs.(5) and (6), eq.(1) becomes

$$\frac{\partial u_j}{\partial x_j} = \frac{\alpha}{\mathrm{C_p}}\frac{\partial}{\partial x_j}\left(\kappa\frac{\partial T}{\partial x_j}\right). \tag{7}$$

Since Coriolis and buoyancy force act on the flow, the external force in eq.(2) is

$$\boldsymbol{K} = (2\Omega u_2,\ -2\Omega u_1,\ \alpha g\Delta T).$$

Ω : angular velocity of the rotation of the earth, $\Delta T = T - T_b$, T_b : base temperature.

Finally, the basic equations in this study are

$$\frac{\partial u_j}{\partial x_j} = \frac{\alpha}{\mathrm{C_p}}\frac{\partial}{\partial x_j}\left(\kappa\frac{\partial T}{\partial x_j}\right), \tag{8}$$

$$\frac{\partial u_i}{\partial t} + u_j\frac{\partial u_i}{\partial x_j} = -\alpha T\frac{\partial p}{\partial x_i} + \alpha T\frac{\partial}{\partial x_j}\left\{\mu\left(\frac{\partial u_i}{\partial x_j} + \frac{\partial u_j}{\partial x_i}\right)\right\} + K_i \quad (i = 1, 2, 3), \tag{9}$$

$$\frac{\partial T}{\partial t} + u_j\frac{\partial T}{\partial x_j} = \frac{\alpha T}{\mathrm{C_p}}\frac{\partial}{\partial x_j}\left(\kappa\frac{\partial T}{\partial x_j}\right). \tag{10}$$

$\alpha = \mathrm{R}/p_m$, $\mathrm{C_p}$: specific heat at constant pressure.

The parameters μ and κ are assumed to be constant for simplicity in this study.

These equations are solved by using projection method[6]. This method can be written in the following form when it is applied to the above equations:

$$\boldsymbol{\omega} + \alpha T\mathrm{grad}p = \boldsymbol{F}, \tag{11}$$

$$\mathrm{div}\boldsymbol{\omega} - \frac{\partial}{\partial t}\left\{\frac{\alpha}{\mathrm{C_p}}\frac{\partial}{\partial x_j}\left(\kappa\frac{\partial T}{\partial x_j}\right)\right\} = 0, \tag{12}$$

where

$$\boldsymbol{F} = F_i, \quad \boldsymbol{\omega} = \omega_i \quad (i = 1, 2, 3),$$

$$\omega_i = \frac{\partial u_i}{\partial t}, \tag{13}$$

$$F_i = -u_j \frac{\partial u_i}{\partial x_j} + \alpha T \frac{\partial}{\partial x_j} \left\{ \mu \left(\frac{\partial u_i}{\partial x_j} + \frac{\partial u_j}{\partial x_i} \right) \right\} + K_i. \tag{14}$$

This suggests that the following decomposition[5] instead of the Helmholtz's decomposition works for the flow with high temperature difference:

$$\boldsymbol{\omega}^n = \boldsymbol{F} - \alpha T \mathrm{grad} p^n, \tag{15}$$

$$p^{n+1} = p^n - \varepsilon \left[\mathrm{div}\boldsymbol{\omega}^n - \frac{\partial}{\partial t} \left\{ \frac{\alpha}{C_p} \frac{\partial}{\partial x_j} \left(\kappa \frac{\partial T}{\partial x_j} \right) \right\} + \frac{1}{\Delta t} \left\{ \frac{\partial u_j}{\partial x_j} - \frac{\alpha}{C_p} \frac{\partial}{\partial x_j} \left(\kappa \frac{\partial T}{\partial x_j} \right) \right\} \right], \tag{16}$$

where the index n denotes the nth iterations and ε is a relaxation constant. The last term bracketed by a parenthesis in eq.(16) is the correction term for preventing the accumulation of the error in $\boldsymbol{\omega}$ [6]. If p and ε are regarded as the temperature and time increment, eq.(16) is considered to be the heat equation discretized by the Eular explicit method. Eq.(16) becomes Poisson equation for the pressure

$$\begin{aligned} 0 = \frac{\partial}{\partial x_j} \left(\alpha T \frac{\partial p}{\partial x_j} \right) - \frac{\partial}{\partial x_k} \left[-u_j \frac{\partial u_k}{\partial x_j} + \alpha T \frac{\partial}{\partial x_j} \left\{ \mu \left(\frac{\partial u_k}{\partial x_j} + \frac{\partial u_j}{\partial x_k} \right) \right\} + K_k \right] \\ + \frac{\partial}{\partial t} \left\{ \frac{\alpha}{C_p} \frac{\partial}{\partial x_j} \left(\kappa \frac{\partial T}{\partial x_j} \right) \right\} - \frac{1}{\Delta t} \left\{ \frac{\partial u_j}{\partial x_j} - \frac{\alpha}{C_p} \frac{\partial}{\partial x_j} \left(\kappa \frac{\partial T}{\partial x_j} \right) \right\} \end{aligned} \tag{17}$$

after the convergence when p^{n+1} is equal to p^n. Although this method is essentially the same as the MAC method, the effect of the compressibility due to the temperature difference is correctly evaluated in this formulation.

Three-dimensional thermal-flow problems with the hook-type heat source are solved in a domain shown in fig.1. Temperature of the heat source is kept to the constant value of T_h, where T_h is 373K while the temperature of the ambient air is set to 273K.

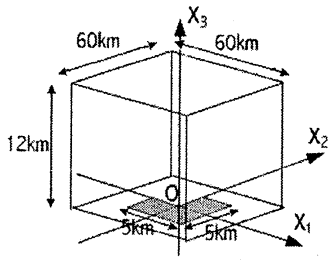

Fig.1. Computational domain, using Descartes coordinates system.

Boundary conditions in this computation are as follows:

Top $\quad \dfrac{\partial u}{\partial z} = 0, \ \dfrac{\partial v}{\partial z} = 0, \ w = 0, \ \dfrac{\partial T}{\partial z} = 0, \ \dfrac{\partial p}{\partial z} = \mu \dfrac{\partial^2 w}{\partial z^2} + \dfrac{K_z}{\alpha T}$

Far distance $\quad u = 0, \ v = 0, \ w = 0, \ T = T_b,$ $\begin{cases} \dfrac{\partial p}{\partial x} = \mu \dfrac{\partial^2 u}{\partial x^2} + \dfrac{K_x}{\alpha T} \\ \text{or} \\ \dfrac{\partial p}{\partial y} = \mu \dfrac{\partial^2 v}{\partial y^2} + \dfrac{K_y}{\alpha T} \end{cases}$

Ground $\quad u = 0, \ v = 0, \ w = 0, \ T = \begin{cases} T_h & \text{(on the heat source)} \\ T_b & \text{(elsewhere)} \end{cases},$

$$\frac{\partial p}{\partial z} = \mu \frac{\partial^2 w}{\partial z^2} + \frac{K_z}{\alpha T}.$$

Non-uniform grid which is strongly concentrated near the heat source is used in this computation (fig.2). The number of the grid points is 97×97×49.

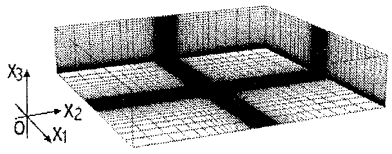

Fig.2. Computational grids.

The non-linear term is approximated by the third-order upwind scheme. The other spatial derivatives are approximated by the central differences. The second-order Crank-Nicolson implicit scheme is used for the time integration.

Parameters used in this study are as follows:

$\mu(\mathrm{kg \cdot m^{-1}s^{-1}})$	:	17.0×10^{-6} $\rightarrow$ 17.0(eddy viscosity)
$\kappa(\mathrm{m^2s^{-1}})$	:	18.0×10^{-6} $\rightarrow$ 18.0(turbulent thermal diffusion)
$\mathrm{C_p}$	:	1.0
$\Omega(\mathrm{rad \cdot s^{-1}})$	:	3.8×10^{-5}
$g(\mathrm{m \cdot s^{-2}})$	:	9.8
$T_b(\mathrm{K})$	:	273
$T_h(\mathrm{K})$	:	373
$\alpha(\mathrm{K^{-1}})$	:	$1/T_b$

III. Results

Numerical computation was carried out for the flow with fire tornado induced by a big fire. The results of the computation are visualized from various viewpoints.

(1) Volume rendering technique is used for the expression of the temperature field. Fig.3(a) and (b) show the results of 500 sec and 2000 sec after the heating. Many thermal plumes appear in fig.3(b). The fire tornado is observed at 5000 sec (fig.3(c)). However, it starts to break down at 7300 sec ((d)) and the tornado disappears eventually around 9000sec ((e),(f)). If the heat is supplied continuously at the heat source, nearly the same phenomena are observed after the breakdown, i.e. the fire tornado is reformed ((h)) after many plumes reappear ((g)) and it breaks down once again ((i),(j)).

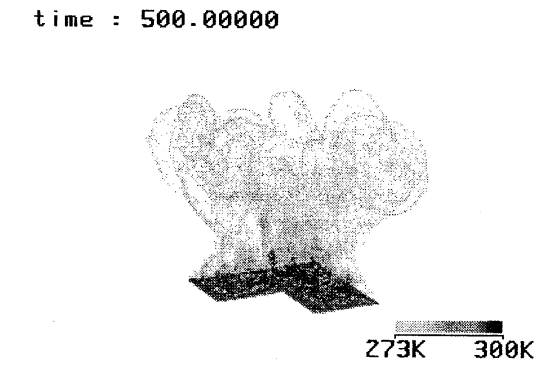
time : 500.00000
273K
300K

(a)

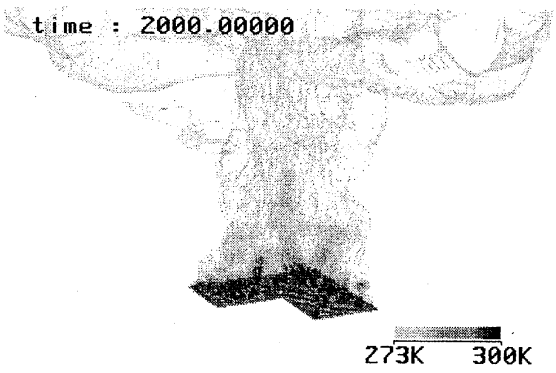
time : 2000.00000
273K
300K

(b)

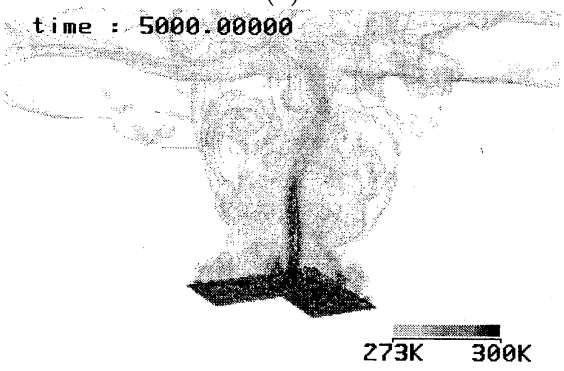
time : 5000.00000
273K
300K

(c)

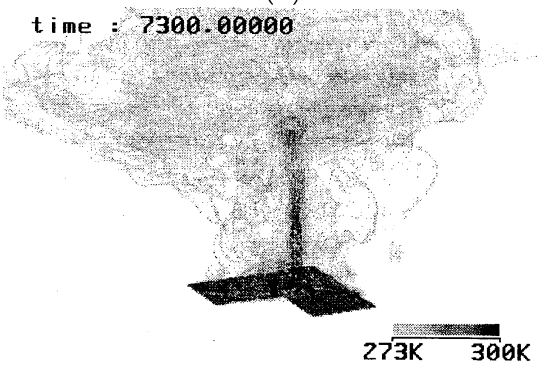
time : 7300.00000
273K
300K

(d)

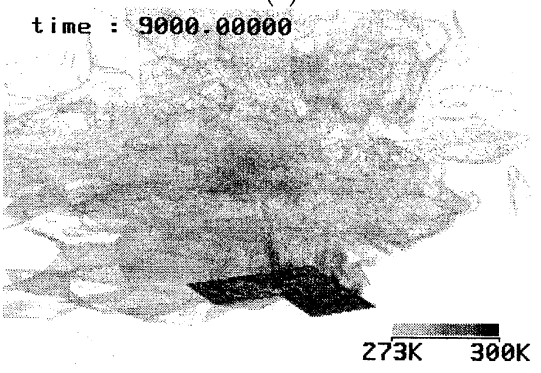
time : 9000.00000
273K
300K

(e)

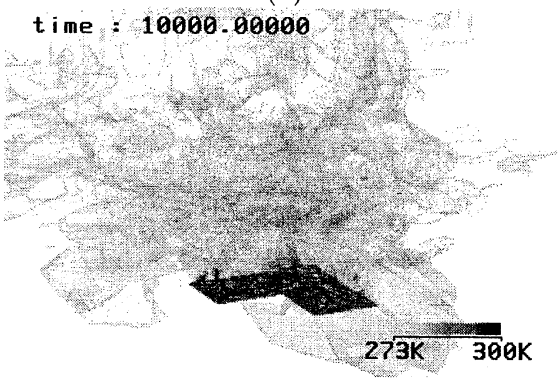
time : 10000.00000
273K
300K

(f)

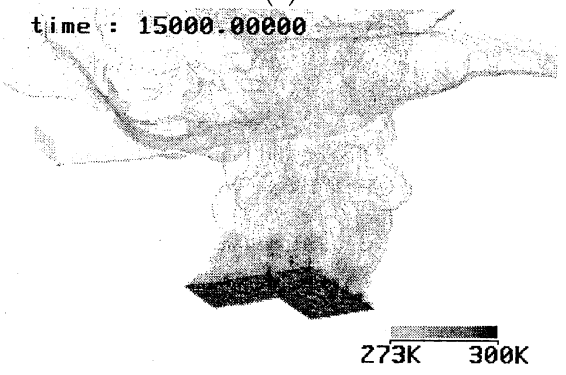
time : 15000.00000
273K
300K

(g)

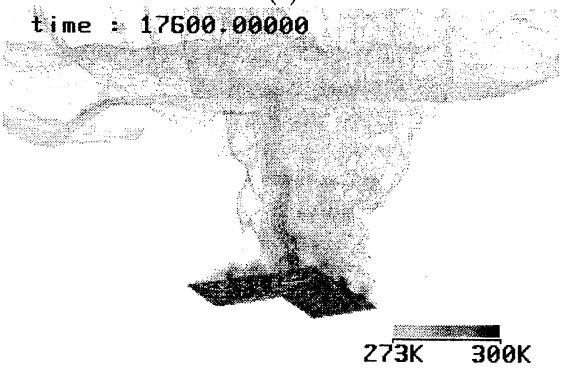
time : 17600.00000
273K
300K

(h)

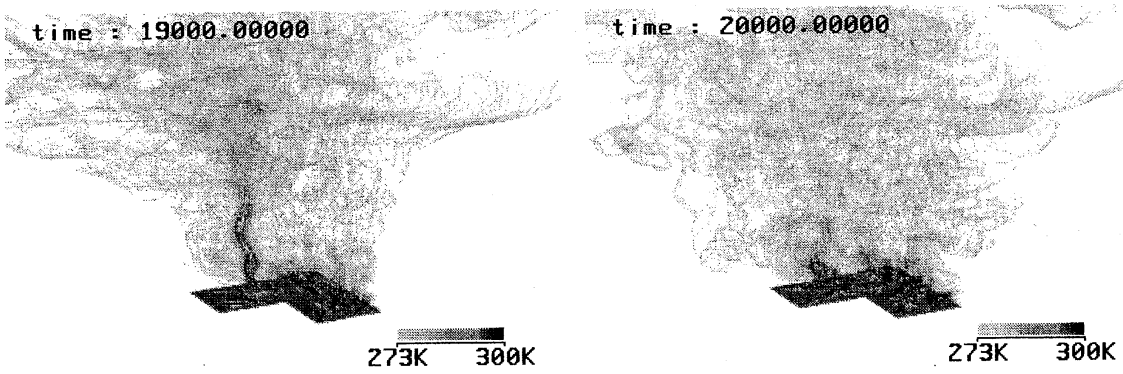

(i) (j)

Fig.3. Time development of temperature fields by volume rendering technique. Time is expressed in seconds.

(2) Details of the flow fields at the time of the vortex breakdown are shown in figs.4,5. These figures show the results at two different times i.e. when the tornado just starts to break down (fig.4) and when it disappears after the breakdown (Fig.5). Figs.4(a),5(a) are the absolute value of the vorticity expressed by the volume rendering technique and stream lines from the heat source. Figs.4(b),5(b) are the pressure shading on the ground and a equi-pressure contour surface. In fig.4, it is clear that strong vorticity appears on the ground when the vortex breakdown just starts. On the other hand, there is no vorticity region before the vortex breakdown. In fig.5, strong vorticity appears locally near the heat source. Additionally, the region of high pressure is localized inside of the region where the strong vorticity is observed.

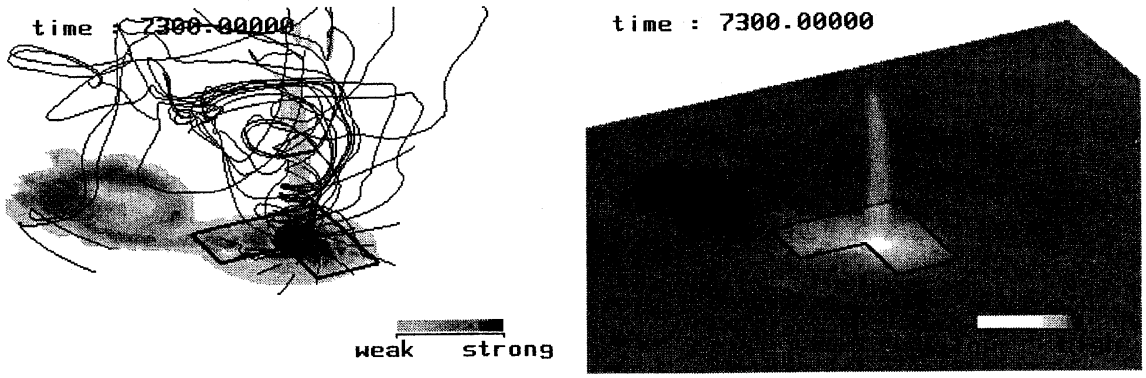

(a) (b)

Fig.4. The tornado just starts to break down. Vorticity and stream lines (a), and pressure field (b).

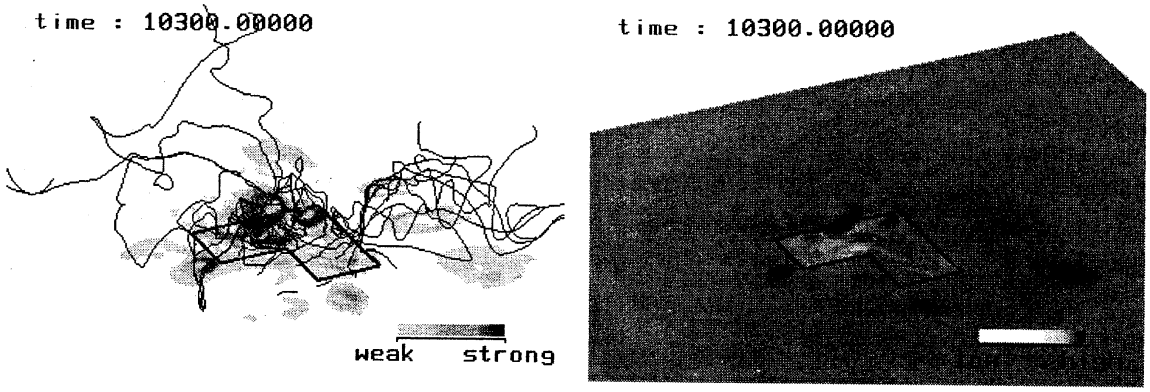

(a) (b)

Fig.5. The tornado disappears after the break down. Vorticity and stream lines (a), and pressure field (b).

(3) Velocity fields are investigated at the time when the strong vorticity regions appear on the ground (fig.6). Two kinds of a contour surface of vertical velocity are drawn in addition to shading of the vorticity on the ground. In this figure, the light-gray and dark-gray surfaces indicate +15m/s and -15m/s respectively. Fig.6(a),(d) are the results before and after the breakdown of the tornado and (b),(c) are those during the breakdown. In fig.6, it is observed that impinging jets toward the ground appear at the time of the breakdown and they induce the strong vorticity on the ground.

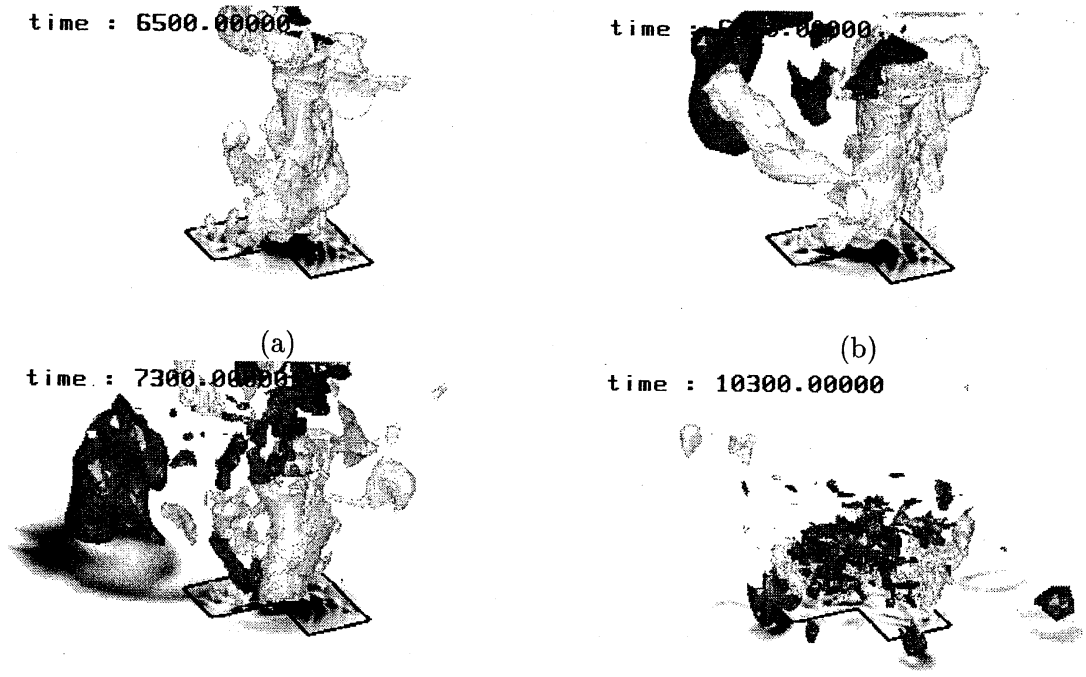

(a) (b)

(c) (d)

Fig.6. Shading of the vorticity on the ground and two kinds of a contour surface of vertical velocity. The light-gray and dark-gray surfaces indicate +15m/s and -15m/s respectively.

IV. Conclusions

The thermal convection induced by the hook-type heat source was simulated. The temperature of the heat source is 100 ℃ higher than the base temperature. Parameters and the boundary conditions employed in this study were chosen to represent the realistic situation which might have occured in the Great Kanto Earthquake. As the result of the computation with Coriolis force, it is found that fire tornados are generated after the thermal convection without a strong rotation is formed by the heat source on the ground. The vortices strongly concentrate so that they become a single vortex. After this concentration, the vortex breakdown takes place and the tornado disappears eventually.

This process is repeated when the heat is continuously supplied from the heat source, i.e. the fire tornado is reformed, breaks down and disappears once again. Particularly, strong vorticity is found on the ground just after the breakdown. It is found that the high pressure region is localized on the ground. This region coincides with that of strong vorticity. It is generated by the downwashes which are formed at the vortex breakdown.

This is the one of the probable stories which took place in the calamity at the Great Kanto Earthquake.

References

1) S.Soma: Study on the Fire-Tornado at the Former Site of the Hifukusho (the Army Clothing Depot), J. Geography 84(1975), p.12
2) K.Kuwahara and Y.Oshima: Thermal Convection Caused by Ring-Type Heat Source, Journal of the Physical Society of Japan, Vol.51, No.11(1982), p.3711
3) H.Suito, K.Kuwahara and K.Satoh: Simulation of Fire Tornado Proc. of 1995 Japan Society for Safety Engineering(1995), p.129
4) K.Sato: Numerical Study and Experiments of Fire Whirl, Proc. INTERFLAM(1996), p.393
5) K.Kuwahara: Computation of Thermal Convection with a Large Temperature Difference, Proc. International Conf. on Applied Numerical Modeling(1984)
6) H.Takami and K.Kuwahara: Numerical Study of Three-Dimensional Flow within a Cubic Cavity, Journal of the Physical Society of Japan, Vol.37, No.6(1974), p.1695
7) S.Komurasaki, T.Kawamura and K.Kuwahara: Numerical Simulation of the Formation of Fire Tornado, Proc. of 11th Computational Fluid Dynamics Symposium(1997), p.491
8) S.Komurasaki, T.Kawamura and K.Kuwahara: Vortex Breakdown in Fire Tornado, Proc. of 12th Computational Fluid Dynamics Symposium(1998), p.401